1490 *J. Am. Chem. Soc.* **1993**, *115*, 1490–1495

Fundamental Frequencies Increasing with Reduced Masses: An Inverse Quantum Isotope Effect in Molecules with Shallow Double-Well Potentials, E.g. Semibullvalenes

K. Bergmann,[§] S. Görtler,[§] J. Manz,*,[†] and H. Quast[‡]

Contribution from the Institut für Physikalische Chemie and the Institut für Organische Chemie, Universität Würzburg, W-8700 Würzburg, Germany. *Received March 10, 1992*

Abstract: We predict an inverse quantum isotope effect for molecules that may isomerize in a shallow double-well potential. Here the corresponding fundamental vibrational transition may excite a delocalized state with energy just above the potential barrier. In this case, increasing molecular masses is predicted to yield increasing fundamental frequencies, in marked contrast to the familiar opposite trend in other molecules. The novel effect is illustrated for simple models representing symmetric semibullvalenes, consistent with experimental values for the relevant masses, bond lengths, and NMR and UV spectra. The effect is explained in terms of illuminating approximations, i.e., harmonic oscillators for the potential wells and a square well for the domain of the potential barrier. Turning the table, we predict that observations of the novel effect indicate shallow double-well potentials with barrier heights slightly below the level which is excited by the fundamental transition.

1. Introduction

Isotopic substitution in molecules usually *decreases* the relevant fundamental vibrational frequencies (ω) with *increases* in molecular mass (more specifically, the reduced mass, μ). This "ordinary" quantum isotope effect is often explained in terms of simple models, such as the ubiquitous harmonic oscillator where $\omega \sim \mu^{-1/2}$, or $\omega \sim \mu^{-1}$ for the case of the square well. This effect has been confirmed experimentally for many molecules.[1]

In this paper, we predict the occurrence of an "inverse" quantum isotope effect, an interesting exception to the general rule: The fundamental frequency may *increase* with molecular mass in molecules with double-well potentials V, where the wells are separated by a relatively low barrier $V^{\neq}$. Typically, these shallow double wells represent the isomerization reaction A $\rightleftarrows$ B, in which the exceptional fundamental frequency ω is associated with the vibration along the reaction coordinate q.

This novel effect is demonstrated below for a simple one-dimensional model of symmetric semibullvalenes with a double-well potential $V_n(q)$ (section 2). The isomerization A $\rightleftarrows$ B corresponds to a Cope rearrangement, in which the appropriate barrier height $V^{\neq}$ is obtained by making the proper substitutions on selected semibullvalenes or derivatives.[2-5] Our one-dimensional model for the specific case of semibullvalenes is explained in the Appendix. However, the predicted effect is general, and, therefore, it should be applicable to other molecules with similar shallow double-well potentials. We also compare our model with that of a shallow double-well potential that yields the ordinary isotope effect, $V_b(q)$. The differences in behavior of $V_n(q)$ and $V_b(q)$ reveal some of the important criteria required for producing the inverse isotope effect.

In order to explain the inverse isotope effect, we employ a combination of simple models which yield the normal isotope effect (e.g., harmonic oscillators and the square well representing approximately the wells and the barrier region of the shallow double-well potential). The discussion about this subject appears in section 3, and conclusions are drawn in section 4.

2. Models and Techniques

Scheme I. Cope rearrangement of model semibullvalene versus reaction coordinate q (schematic)

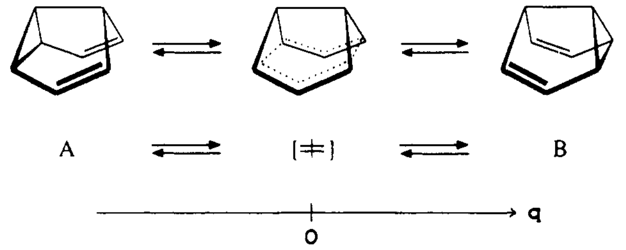

Table I. Model Potentials for Semibullvalenes

parameter[a]	V_b	V_n
V_0/kJ mol^{-1}	25.1[b]	25.1[b]
V_0/E_h	0.009562	0.009562
V_2/E_h	−0.01922	−0.01922
V_4/E_h	0.009564	0.009564
q_e/a_0	0.6246[c]	0.6246[c]
n	0.7931	2.662
$k/(E_h a_0^{-2})$	0.1232	1.385
$\hbar\omega/E_h$	0.004103	0.004105
$\hbar\omega$/cm^{-1}	900.6[d]	900.9[d]

[a] See eqs A7 and A8. [b-d] Experimental references[21-23]: (b) ca. 25 kJ mol^{-1}, (c) >0.624a_0, (d) ca. 900 cm^{-1}.

We consider in our model systems two symmetric, shallow double-well potentials $V(q)$ as representative of the vibrations of equivalent molecular isomers, A and B (e.g., semibullvalenes; see Appendix), along the A $\rightleftarrows$ B isomerization coordinate q, with a reduced mass μ. The two potentials share several properties, but they also differ in some aspects important for observing the novel isotope effect. The potentials are shown in Figures 1 and 2 with the energy levels E_v and wave functions $\langle q|v\rangle = \Psi_v(q)$ of different vibrational states $|v\rangle = |0\rangle, |1\rangle, |2\rangle$, for two different masses (μ

[†] Institut für Physikalische und Theoretische Chemie, Freie Universität Berlin, Takustr. 3, D-1000 Berlin 33.

[§] Institut für Physikalische Chemie.

[‡] Institut für Organische Chemie.

(1) Herzberg, G. *Molecular Spectra and Molecular Structure. I. Spectra of Diatomic Molecules*; Van Nostrand Reinhold: New York, 1950; pp 73–81, 141–145, 162–168. Herzberg, G. *Molecular Spectra and Molecular Structure. II. Infrared and Raman Spectra of Polyatomic Molecules*; Van Nostrand Reinhold: New York, 1945; pp 227–238.

(2) For pioneering work on the degenerate Cope rearrangement of semibullvalene, see: Zimmerman, H. E.; Grunewald, G. L. *J. Am. Chem. Soc.* **1966**, *88*, 183–184. Zimmerman, H. E.; Binkley, R. W.; Givens, R. S.; Grunewald, G. L.; Sherwin, M. A. *Ibid.* **1969**, *91*, 3316–3323.

(3) Theoretical studies of the barriers toward the degenerate Cope rearrangement of semibullvalenes: Dewar, M. J. S.; Schoeller, W. W. *J. Am. Chem. Soc.* **1971**, *93*, 1481–1482. Hoffmann, R.; Stohrer, W.-D. *Ibid.* **1971**, *93*, 6941–6948. Dewar, M. J. S.; Lo, D. H. *Ibid.* **1971**, *93*, 7201–7207. Iwamura, H.; Morio, K.; Kunii, T. L. *Bull. Chem. Soc. Jpn.* **1972**, *45*, 841–846. Miller, L. S.; Grohmann, K.; Dannenberg, J. J. *J. Am. Chem. Soc.* **1983**, *105*, 6862–6865. Dewar, M. J. S.; Jie, C. *Tetrahedron* **1988**, *44*, 1351–1358. Williams, R. V.; Kurtz, H. A. *J. Org. Chem.* **1988**, *53*, 3626–3628.

(4) Determination by nuclear magnetic resonance spectroscopy of the barriers toward the degenerate Cope rearrangement of semibullvalenes: (a) Cheng, A. K.; Anet, F. A. L.; Mioduski, J.; Meinwald, J. *J. Am. Chem. Soc.* **1974**, *96*, 2887–2891. (b) Moskau, D.; Aydin, R.; Leber, W.; Günther, H.; Quast, H.; Martin, H.-D.; Hassenrück, K.; Miller, L. S.; Grohmann, K. *Chem. Ber.* **1989**, *122*, 925–931.

0002-7863/93/1515-1490$04.00/0

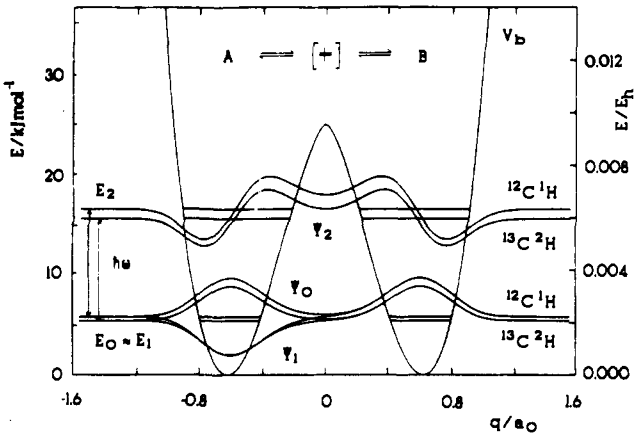

Figure 1. Model potential V_b versus reaction coordinate q for the Cope rearrangement of model semibullvalene (cf. Scheme I), together with the energies $E_0 < E_1 < E_2$ for light (^{12}C^{1}H) and heavy (^{13}C^{2}H) isotopomers, and energies of the fundamental transition $\hbar\omega = E_2 - E_0$. Superimposed are the wave functions Ψ_0, Ψ_1, Ψ_2, with their asymptotes running into the respective energy levels, E_0, E_1, E_2, in the right- and left-hand sides of the figure.

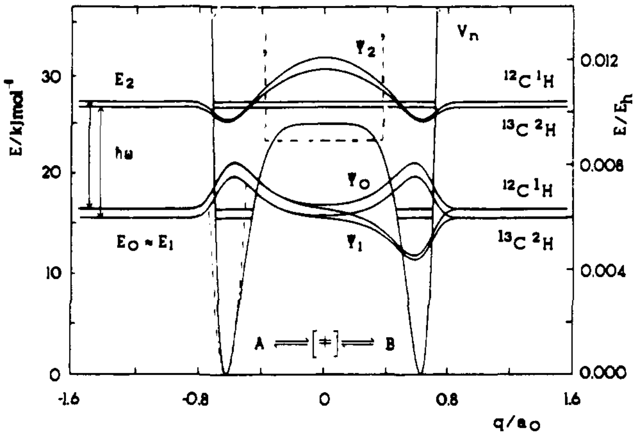

Figure 2. Model potential V_n of semibullvalenes, with properties as in Figure 1. Approximate harmonic and square-well potentials for the wells and barrier region of V_n are indicated by dashed lines.

= 13/4 u and μ = 15/4 u, where 1 u = 1.66054 × 10^{-27} kg = unified atomic mass unit). The E_v and $\Psi_v(q)$ are evaluated by solving the Schrödinger equation

$$\left[-\frac{\hbar^2\partial^2}{2\mu\partial q^2} + V(q)\right]\Psi_v(q) = E_v\Psi_v(q) \qquad (1)$$

by the Numerov method[6] with atomic units. The symmetry of the potential

$$V(q) = V(-q) \qquad (2)$$

implies that the symmetries of successive $\Psi_v(q)$ alternate between gerade (+) and ungerade (−) symmetries, and there are v nodes for $\Psi_v(q)$. The energies E_0, E_1 of states $|0\rangle$, $|1\rangle$ are near-degenerate. The very small energy gap $E_1 - E_0$ (below the graphical resolutions of Figures 1 and 2) determines the time τ for tunneling through the potential barrier by the uncertainty relationship

$$\Delta E\tau = (E_1 - E_0)\tau \simeq h \qquad (3)$$

In contrast to the tunneling transition $|0\rangle \rightarrow |1\rangle$, the transition $|0\rangle \rightarrow |2\rangle$ is defined as the fundamental transition of isomers A or B. This definition is based on the reference case of large barriers separating A and B into nearly isolated isomers. In this instance, the first excited states $|1\rangle$ of the individual isomers correspond to the second excited state $|2\rangle$ of the interactive A and B. Therefore, upon decreasing the barrier height from large to low values, the $|0\rangle \rightarrow |1\rangle$ fundamental transitions of the individual isomers approach the $|0\rangle \rightarrow |2\rangle$ transition of the interacting A and B.

Some important common properties of the two potentials are shown in Figures 1 and 2. Particularly, both potentials are scaled to zero at the equivalent potential minima for isomers A and B, and both have the same barrier height V^* and the same photon energies for the fundamental transition:

$$\hbar\omega = E_2 - E_0 \qquad (4)$$

The potentials have different force constants, which yield either broad ("b") or narrow ("n") widths of the potential wells. Therefore, the two potentials shown in Figures 1 and 2 are labeled $V_b(q)$ and $V_n(q)$, respectively. Note that for $V_b(q)$, all energies $E_0 - E_2$ are below the barrier height V^*, and the corresponding wavepackets $\Psi_0(q) - \Psi_2(q)$ are localized within the potential wells. The same behavior is observed for the states $|0\rangle$ and $|1\rangle$ of $V_n(q)$. In contrast, the E_2 energy level lies above the potential barrier V^*, and $\Psi_2(q)$ is rather delocalized. The maximum density appears at the top of the barrier and not in the domains of the wells of $V_n(q)$. The different behaviors,

$$E_2 < V^* \text{ for } V_b(q) \qquad (5a)$$

$$E_2 > V^* \text{ for } V_n(q) \qquad (5b)$$

will produce either the "normal" or the "inverse" isotope effects.

The computations were carried out on a Sun SPARCstation computer.

3. Results and Discussion

Substituting atoms in molecules by heavier isotopes decreases the vibrational energies E_v. This general rule also holds for the present model systems with shallow double-minimum potentials. For example, substituting the ^{12}C^{1}H bonds in semibullvalenes with ^{13}C^{2}H bonds not only increases the reduced mass μ from (12 + 1)/4 u to (13 + 2)/4 u (Appendix), but also decreases the corresponding energy levels E_v (Figures 1 and 2). However, both qualitative and quantitative differences are seen in the isotopic shifts of levels $E_0 - E_2$ for $V_b(q)$ and $V_n(q)$. Specifically, for $V_b(q)$, the shift of level E_0 is smaller than that for E_2, and hence the transition frequency (eq 4), decreases with mass. The opposite trend occurs for $V_n(q)$. We explain this using the following simple models.

Consider first the "ordinary" isotope effect observed in the case of $V_b(q)$ (Figure 1), in which $E_2 < V^*$ (eq 5a). Both the $|0\rangle$ and $|2\rangle$ states are embedded in the potential wells. In the harmonic approximation for individual isomers A and B, these potential wells may be expanded at their equilibrium positions (q_e) as

$$V_b(q) \approx 0.5k_b(q \pm q_e)^2 \qquad (6a)$$

with force constant

$$k_b = \partial^2V_b/\partial q^2 \text{ at } q = \pm q_e \qquad (6b)$$

As a consequence,

$$E_0 \simeq 0.5\hbar\omega_b \qquad (7a)$$

$$E_2 \simeq 1.5\hbar\omega_b \qquad (7b)$$

$$\omega_b = (k_b/\mu)^{1/2} \qquad (7c)$$

and the energy gap decreases with reduced mass (μ) according to the following relation

$$\hbar\omega = E_2 - E_0 \simeq \hbar\omega_b = \hbar(k_b/\mu)^{1/2} \qquad (7d)$$

Consider now the extraordinary properties of $V_n(q)$ (Figure 2).

---

(5) (a) Quast, H.; Christ, J.; Peters, E.-M.; Peters, K.; von Schnering, H. G. *Chem. Ber.* **1985**, *118*, 1154–1175. (b) Quast, H.; Mayer, A.; Peters, E.-M.; Peters, K.; von Schnering, H. G. *Ibid.* **1989**, *122*, 1291–1306.

(6) Press, W. H.; Flannery, B. P.; Teukolsky, S. A.; Vetterling, W. T. *Numerical Recipes*; Cambridge University Press: Cambridge, 1989; pp 356–363.

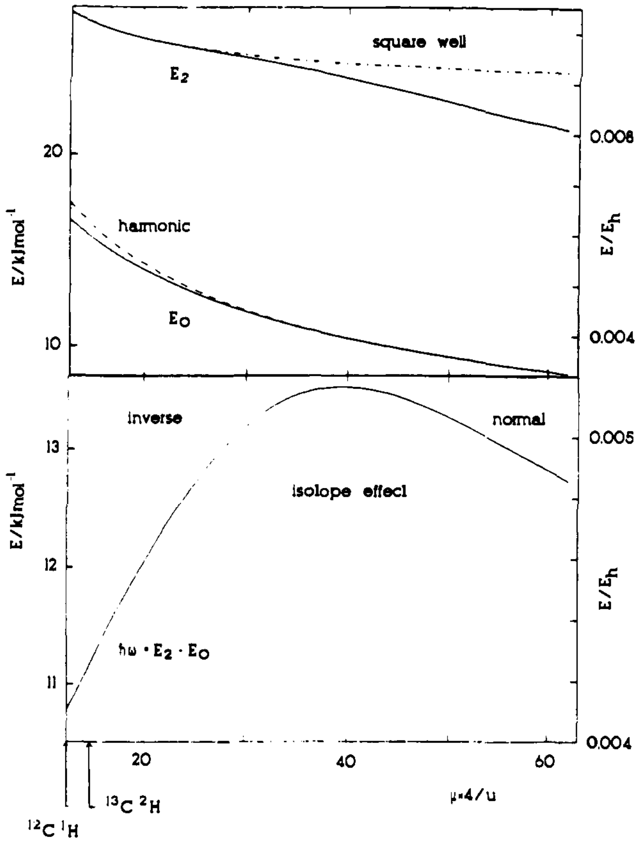

Figure 3. Energies of levels E_0, E_2 and of the fundamental transition $\hbar\omega = E_2 - E_0$ versus reduced mass $\mu \times 4$, compared with the results for the harmonic and square-well model potentials; see Figure 2.

The vibrational ground state $|0\rangle$ is also embedded in the near-harmonic potential wells,

$$V_n(q) \approx 0.5k_n(q \pm q_e)^2 \quad (8a)$$

with force constant

$$k_n = \partial^2 V_n/\partial q^2 \text{ at } q = \pm q_e \quad (8b)$$

Therefore,

$$E_0 \simeq 0.5\hbar\omega_n = 0.5\hbar(k_n/\mu)^{1/2} \quad (9a)$$

in analogy to eqs 6, 7a, and 7c. The $E_0 \sim \mu^{-1/2}$ relationship (9a) is illustrated in Figure 3. This expression is valid in the limiting cases of heavy masses, in which E_0 decreases to the potential minima where the harmonic approximation (8a) is perfect. Figure 3 shows the validity of the asymptotic relation $E_0 \sim \mu^{-1/2}$ for the relatively light reduced masses of semibullvalene isotopomers, $\mu \sim 13/4$ u.

In contrast to E_0, the excited energy E_2 of $V_n(q)$ lies *above* the potential barrier (eq 5b), and the harmonic model (eq 7b) is invalid. The barrier region of $V_n(q)$, occurring between the potential minima $V_n(\pm q_e)$, can be approximated by a square-well model with the effective length L

$$L < 2q_e \quad (10a)$$

and with a minimum potential slightly below the barrier height,

$$V_m \lesssim V^* \quad (10b)$$

(Figure 2). In this example, E_2 should be close to the zero-point energy,

$$E_2 \simeq V_m + \hbar^2\pi^2/(2\mu L^2) \quad (9b)$$

and $\Psi_2(q)$ for the square-well domain should resemble the ubiquitous sinusoidal wave function with some perturbations (e.g., nodal structures), which are caused by the adjacent wells of $V_n(q)$ (Figure 2). The $E_2 - V_m \sim \mu^{-1}$ relationship (9b) is also illustrated in Figure 3. It is accurate in the limit of light masses μ, in which the level E_2 is shifted more up and away from any "perturbing effects" of the wells of $V_n(q)$. Figure 3 also shows that the $E_2 - V_m \sim \mu^{-1}$ relationship is valid for the reduced masses of the light semibullvalene isotopomers, $\mu \gtrsim 13/4$ u, for the parameter values

$$V_m = 23.4 \text{ kJ mol}^{-1} \text{ and } L = 0.75a_0$$

For comparison, we also consider the hypothetical case of much heavier masses $\mu > 30/4$ u. In this case, E_2 is expected to decrease below the potential barrier V, and $\Psi_2(q)$ would ultimately be trapped in near harmonic potential wells, similar to the case of $V_b(q)$ (eq 7b). The corresponding breakdown of the $E_2 - V_m \sim \mu^{-1}$ relationship for $\mu > 30/4$ u is illustrated in Figure 3, together with the harmonic limit (eq 7b) which would be established for $\mu > 50/4$ u.

The inverse isotope effect arises as a consequence of the different "harmonic" and "square-well" mass dependences of E_0 and E_2 (eqs 9a and 9b, respectively). The decrease of E_0 with mass μ (eq 9a) is more pronounced than the decrease of E_2 (eq 9b), and, therefore, the energy gap

$$\hbar\omega = E_2 - E_0 \simeq V_m + \hbar^2\pi^2/(2\mu L^2) - 0.5\hbar[(\partial^2 V_n/\partial q^2)/\mu]^{1/2} \quad (11)$$

increases with mass μ. Thus, eq 11 represents the quantum isotope effect, which is illustrated in the bottom panel of Figure 3. The ordinary isotope effect (eq 7d) occurs for masses $\mu \gtrsim 40/4$ u when the criterion $E_2 > V^*$ (eq 5b) is changed into $E_2 < V^*$ (eq 5a). Then the square-well behavior of relationship 9b is converted to the harmonic in analogy with eqs 7b and 7c.

The explicit relationship 11 indicates that the inverse isotope effect would be further enhanced by additional isotopic mass scalings of the coordinate q and the corresponding domain L of the potential barrier,

$$\begin{aligned} q &\rightarrow f \times q \\ L &\rightarrow f \times L \end{aligned} \quad (12)$$

in which f is a factor which increases with mass. This type of substitution (12) may arise in semibullvalenes, when the $^{12}C^1H$ bonds are substituted by $^{13}C^2H$. Consequently, the centers of mass of the $\overline{\mathrm{CH}}$ bonds would move from C toward H, causing the stretch in relationship 12 of q and L (eqs A1, A2).

4. Conclusions

Experimental results such as bond lengths, and NMR, and UV spectra of semibullvalenes are compatible with the depiction of the potential as a shallow double well (Figure 2). Subsequently, the shape of the potential yields the inverse isotope effect. Although the experimental results are suggestive of this effect in some semibullvalenes, the ultimate proof by high resolution IR or Raman spectroscopy is still pending.

We predict the following criterion for observing the novel inverse isotope effect by extrapolating the results for the simple model semibullvalenes of section 2 and 3. Accordingly, the molecules should have shallow double-well potentials supporting two isomers such that the vibrational ground state Ψ_0 is embedded in the potential wells with energy below the potential barrier, $E_0 < V^*$, and the excited state Ψ_2 is delocalized in the domain of the potential barrier, with energy $E_2 > V^*$. Then the fundamental transition frequency ω, or the corresponding photon energy $\hbar\omega = E_2 - E_0$ increases with the reduced mass μ for the vibration along the reaction coordinate q. This criterion is a working hypothesis that is applicable not only to degenerate semibullvalenes, but also to other molecules with similar shallow double-well potentials. Possible candidates include (a) hydrogen-bonded species such as $H_2O\cdots HF$,[7] (b) ring systems with puckered ring skeletal modes such as trimethylene sulfide derivates,[8,9] (c) molecules exhibiting

---

(7) Legon, A. C. *Chem. Soc. Rev.* **1990**, *19*, 197–237.

(8) Harris, D. O.; Harrington, H. W.; Luntz, A. C.; Gwinn, W. D. *J. Chem. Phys.* **1966**, *44*, 3467–3480.

(9) Möller, K. D.; Rothschild, W. G. *Far-Infrared Spectroscopy*; Wiley: New York, 1971; pp 218–302.

internal rotations or torsional motions such as methanol derivatives,[9,10] or hydrogen peroxide,[9,11] and (d) molecules capable of undergoing pyramidal inversions, such as ammonia derivatives,[12] methyl anions,[13] or the hydronium ion.[14] The mentioned molecules or some appropriate derivatives must meet the criterion $E_0 < V^{\ddagger} < E_2$ in order to produce the "inverse" quantum isotope effect. This requires a great deal of selectivity because some systems have E_2 slightly below the barrier (e.g., trimethylene sulfide,[8,9] methanol,[9,10] ammonia,[12] and the hydronium ion[14]), whereas other systems have $E_2 > V^{\ddagger}$ for the light isotopomers (e.g., H_2O_2,[9,11] CH_3^-[13]) but $E_2 < V^{\ddagger}$ for the heavy isotopomers (e.g., D_2O_2,[9,11] CD_3^-[13]). In these cases, the normal isotope effect is reestablished, similar to the switch from the "inverse" to the "normal" isotope effect explained earlier (Figure 3). The criterion $E_0 < V^{\ddagger} < E_2$ should be satisfied for both light *and* heavy isotopomers and requires proper substitutions of the molecules listed above.

Different inverse isotope effects may be exhibited by hydrogen-bonded species such as $H_2O\cdots HF$[7] or by molecules with large amplitude motions, e.g., multimembered rings undergoing inversions, pseudo-rotations, or ring puckering motions.[15] These motions involve substantial bend/stretch coupling, and, as predicted by Bowman et al.[16] for van der Waals complexes of argon atoms and hydroxyl radicals, *all* energy intervals in the stretch progression are larger for Ar⋯DO than for Ar⋯HO. In contrast, the present inverse isotope effect is restricted to the single energy interval, $E_2 - E_0$. This effect could be extended to single energy intervals $E_v - E_{v-1}$ in systems with higher barriers, in which v may also refer to other degrees of freedom, rotations, and vibrations perpendicular to the reaction path. Particularly favorable are systems with a loose transition state such that E_v and E'_w are the ground vibrational states of the transition states for the light (l) and heavy (h) isotopomers, respectively, $E_v = E_{l0}^{\ddagger} > V^{\ddagger} > E_{v-1}$ and $E'_w = E_{h0}^{\ddagger} > V^{\ddagger} > E'_{w-1}$. Because of the low zero-point energies of the loose transition state in this situation, $E_v - E_{v-1}$ may be exceedingly small, and even smaller than the corresponding energy gap $E'_v - E'_{v-1}$ of the heavy isotopomer ($E'_v < V^{\ddagger}$ since $v \ll w$). The spacing between the ground vibrational state of the reactant and that of the transition state is also usually larger for the heavy isotopic species than for the light one, i.e., $E^{\ddagger}_{l0} - E_{l0} < E^{\ddagger}_{h0} - E_{h0}$.

The criterion for producing the inverse isotope effect may be extended to asymmetric systems. For the carrying-through of this procedure, the specific profiles of the potentials must be estimated. Similar to the methods used in the symmetric model, the potentials of asymmetric systems may be approximated by (near-) harmonic potentials for the potential wells, a square-well potential for the domain of the barrier, or other simple models with similar properties (e.g., Morse oscillators, eq A9).

Conversely, we predict that observations of the inverse quantum isotope effect will prove the present criterion

$$E_0 < V^{\ddagger} < E_2 \tag{13}$$

Scheme II. Top view of Cope rearrangement of model semibullvalene versus reaction coordinate q (schematic). For the purpose of this paper, the termini of the allylic parts are labeled by 1-4.

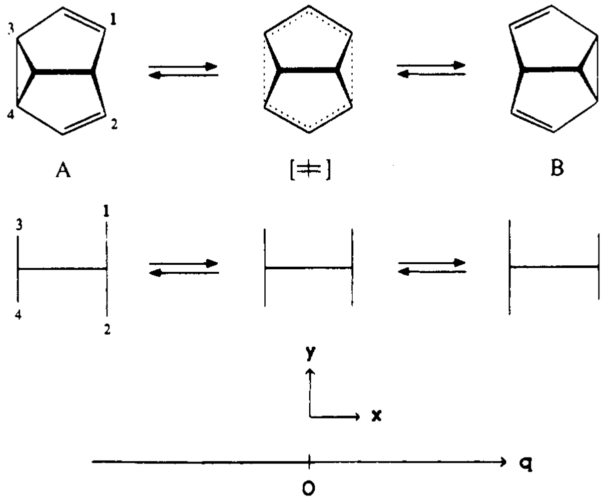

If the value of E_2 is known, this criterion may serve as a semiquantitative method for estimating the potential barrier height, $V^{\ddagger} < E_2$. Alternatively, if $V^{\ddagger}$ can be estimated by means of complementary techniques (see refs 17 and 18), as is the case for semibullvalenes,[4] then eq 13 would yield the relative positions of levels $E_0 < V^{\ddagger}$ and $E_2 > V^{\ddagger}$. We therefore surmise that experiments aimed at confirming the novel quantum isotope effect for molecules with shallow double-well potentials will be both fruitful and rewarding.

Acknowledgment. We express our gratitude to Professors P. Botschwina, Göttingen, W. Kiefer, Würzburg, R. Meyer, Zürich, and Dr. H. U. Suter, Zürich, for suggesting several molecules with shallow double-well potentials as candidates for the present inverse isotope effect. We also thank Dr. C. Doona for editing our manuscript, and Mrs. U. Müller for typing parts of it. Financial support by the Deutsche Forschungsgemeinschaft and the Fonds der Chemischen Industrie is gratefully acknowledged.

Appendix

A rigorous evaluation of the vibrational spectroscopy of semibullvalenes, in particular the fundamental transitions, must be based on the system's Schrödinger equation with the appropriate Hamiltonian representing all nuclei, electrons, and photons. To simplify this formidable task, we invoke the usual approximations, i.e., the Born–Oppenheimer separation of electrons and nuclei, the semiclassical dipole approximation, and the golden rule for dipole-allowed transitions. We also separate vibrational, rotational, and translational motions and assume that the molecule is oriented as indicated in Scheme I. Moreover, we assume a separation of the "active" vibration(s) associated with the Cope rearrangement of the semibullvalenes from all other "passive" ones, also called "promoting modes" and "spectator modes", respectively. Similar separations have been made for isomerizations of other molecules.[18-20]

In the present case, the Cope rearrangement leads from the reactant isomer A via the transition state (‡) to the equivalent product isomer B (see Scheme I), and the "active" vibration(s) are recognized readily from the corresponding top view shown in Scheme II, as follows. Apparently, they involve the carbon atoms labeled C1–C4 which are attached to the bonds (C1–C2) and (C3–C4), together with the hydrogen atoms H1–H4 attached to

---

(10) Burkhard, D. G.; Dennison, D. M. *J. Mol. Spectrosc.* **1959**, *3*, 299–333.

(11) Hunt, R. H.; Leacock, R. A.; Peters, C. W. *J. Chem. Phys.* **1965**, *42*, 1931–1946. Hunt, R. H.; Leacock, R. A. *Ibid.* **1966**, *45*, 3141–3147. Ewig, C. S.; Harris, D. O. *Ibid.* **1970**, *52*, 6268–6271. Dübal, H.-R.; Crim, F. F. *Ibid.* **1985**, *83*, 3863–3872.

(12) Campoy, G.; Palma, A.; Sandoval, L. *Int. J. Quant. Chem.: Quant. Chem. Symp.* **1989**, *23*, 355–361. Bunker, P. R.; Kraemer, W. P.; Spirko, V. *Can. J. Phys.* **1984**, *62*, 1801–1805. Ha, T.-K.; Suter, H. K. Private communication, 1991.

(13) Kraemer, W. P.; Spirko, V.; Malmqvist, P.-A.; Roos, B. O. *J. Mol. Spectrosc.* **1991**, *147*, 526–540.

(14) Botschwina, P. *J. Chem. Phys.* **1986**, *84*, 6523–6524. Maier, J. P. *Ion and Cluster-Ion Spectroscopy and Structure*; Elsevier: Amsterdam, 1989; pp 1–50.

(15) Anderson, J. E. *Top. Curr. Chem.* **1974**, *45*, 139–167. Anet, F. A. L. *Ibid.* **1974**, *45*, 169–220. Carreira, L. A.; Lord, R. C.; Malloy, T. B., Jr. *Ibid.* **1979**, *82*, 1–95. Hollas, J. H. *High Resolution Spectroscopy*; Butterworths: London, 1982; pp 252–267. Laane, J. *Pure Appl. Chem.* **1987**, *59*, 1307–1326.

(16) Bowman, J. M.; Gazdy, B.; Schafer, P.; Heaven, M. C. *J. Phys. Chem.* **1990**, *94*, 2226–2229.

(17) Tang, S. L.; Abramson, E. H.; Imre, D. G. *J. Phys. Chem.* **1991**, *95*, 4969–4976. Tang, S. L.; Imre, D. G. *Ibid.* **1991**, *95*, 4976–4982.

(18) Meyer, R.; Ernst, R. R. *J. Chem. Phys.* **1990**, *93*, 5518–5532.

(19) Makri, N.; Miller, W. H. *J. Chem. Phys.* **1987**, *86*, 1451–1457. Miller, W. H.; Ruf, B. A.; Chang, Y.-T. *Ibid.* **1988**, *89*, 6298–6304.

(20) Frederick, J. H.; Heller, E. J.; Ozment, J. L.; Pratt, D. W. *J. Chem. Phys.* **1988**, *88*, 2169–2184.

C1–C4. The corresponding positions and masses are $R_{C1} - R_{C4}$, $R_{H1} - R_{H4}$ and $m_{C1} - m_{C4}$, $m_{H1} - m_{H4}$, respectively. Let

$$r_i = R_{Hi} - R_{Ci} \tag{A1a}$$

$$R_i = (m_{Ci}R_{Ci} + m_{Hi}R_{Hi})/(m_{Ci} + m_{Hi}) \tag{A1b}$$

denote the corresponding coordinates for the bonds (C_i–H_i), i = 1–4, and their centers of masses, with corresponding Cartesian components x_i, y_i, z_i and X_i, Y_i, Z_i, momenta p_i and P_i, and masses

$$m_i = m_{Ci}m_{Hi}/(m_{Ci} + m_{Hi}) \tag{A1c}$$

$$M_i = m_{Ci} + m_{Hi} \tag{A1d}$$

Then it is obvious from Scheme II that the active, large amplitude motions associated with the Cope rearrangement involve coordinates Y_1–Y_4, and masses M_1–M_4, whereas all other coordinates should describe passive vibrations. Using Y_1–Y_4 and M_1–M_4, we define new variables

$$\begin{aligned} q_1 &= -(Y_1 - Y_2) + (Y_3 - Y_4) \\ q_2 &= (Y_1 - Y_2) + (Y_3 - Y_4) \\ q_3 &= (M_1Y_1 + M_2Y_2)/(M_1 + M_2) - \\ &\qquad (M_3Y_3 + M_4Y_4)/(M_3 + M_4) \\ q_4 &= \Sigma M_iY_i/\Sigma M_i \end{aligned} \tag{A2}$$

with the corresponding momenta $\tilde{p}_i = -i\hbar\partial/\partial q_i$. The q_i have illuminating physical meanings. Essentially, q_1 is the difference of bond lengths (C3–C4) minus (C1–C2), with slight modification from the positions of carbon atoms C1–C4 to the centers of masses of bonds (C1–H1) - (C4–H4). Next, q_2 describes the corresponding sum of modified bond lengths, whereas q_3 is the y component of the modified distance between the centers of masses of bonds (C1–C2) and (C3–C4). Finally, q_4 is the y component of the centers of masses of atoms C1–C4 and H1–H4. Obviously, the Cope rearrangement involves rather large variations of q_1, from negative values for isomer A to corresponding positive ones for B. In contrast, all other variables $q_2 - q_4$ do hardly change during the reaction. In conclusion, our model suggests that q_1 is the promoting mode, whereas all other coordinates describe spectator modes.

For the sake of simplicity, we now separate the molecular vibrational Hamiltonian into two parts,

$$H \simeq H_a + H_p = T_a + T_p + V_a + V_p \tag{A3}$$

with corresponding contributions of the kinetic energies T plus potential energies of the electronic ground state V for the active (a) mode (q_1) plus all other passive (p) ones, neglecting interaction terms $H_{ap} = T_{ap} + V_{ap}$. This decoupling of variables implies, as an approximation, that the active mode q_1 correlates with a normal coordinate Q_1 (with appropriate scalings), and that the fundamental frequency $\omega = \omega_1$ associated with q_1 is determined by the Hamiltonian H_a for q_1. In a more realistic model based, e.g., on a normal mode analysis, q_1 and Q_1 may deviate slightly due to potential coupling V_{ap}, but, for small couplings V_{ap}, this will have only marginal effects on the inverse isotope effect.

For the sake of simplicity, we set $q = q_1$, with corresponding momentum $p = \tilde{p}_1$; thus

$$H_a = p^2/2\mu + V(q) \tag{A4}$$

The reduced mass μ associated with $q = q_1$ is obtained readily by converting the original kinetic energy operator from Cartesian coordinates R_{Ci}, R_{Hi}, R_{Ai} for atoms C_i, H_i, and all other ones A_i into new coordinates,

$$\begin{aligned} T = \sum_{i=1}^{4} P_{Ci}^2/2m_{Ci} + \sum_{i=1}^{4} P_{Hi}^2/2m_{Hi} + \sum_{i=9}^{N} P_{Ai}^2/2m_{Ai} = \\ \sum_{i=1}^{4} P_i^2/2M_i + \sum_{i=1}^{4} p_i^2/2m_i + \sum_{i=9}^{N} P_{Ai}^2/2m_{Ai} = \\ \tilde{p}_1^2/(2M/4) + \tilde{p}_2^2/(2M/4) + \tilde{p}_3^2/2M + \tilde{p}_4^2/(2\times 4M) + \\ \sum_{i=1}^{4} (P_{ix}^2 + P_{iz}^2)/2M_i + \sum_{i=1}^{4} p_i^2/2m_i + \sum_{i=9}^{N} P_{Ai}^2/2m_{Ai} = T_a + T_p \end{aligned} \tag{A5a}$$

where

$$T_a = p^2/2\mu \tag{A5b}$$

$$\text{with } \mu = M/4 \tag{A5c}$$

The third and fourth line in eq A5a holds for symmetric semibullvalenes with equal masses $M_i = m_{Ci} + m_{Hi} = M$. In this case, the separation $T = T_a + T_p$ is rigorous, whereas asymmetric isotopomers would cause some kinetic couplings $T_{ab} \neq 0$. The inverse reduced mass (see eq A5c) may be understood as sum of two reduced masses for the modified bonds (C1–C2) and (C3–C4) vibrating with opposite phases,

$$1/\mu = (M_1 + M_2)/(M_1M_2) + (M_3 + M_4)/(M_3M_4) = 4/M \tag{A5d}$$

The potential energy $V(q) = V_a(q)$ of the active mode $q = q_1$ should represent equivalent isomers A and B; thus

$$V(q) = V(-q) \tag{A6}$$

Accordingly, we assume a flexible, even model function

$$V(q) = V_0 + V_2(q/q_e)^{2n} + V_4(q/q_e)^{4n} \tag{A7}$$

with five parameters, which may be adjusted to satisfy five conditions, as follows. First and second, the potential minima are scaled to zero at their equilibrium values $\pm q_e$,

$$V(q_e) = V(-q_e) = 0 \tag{A8a}$$

$$\partial V/\partial q = 0 \text{ at } q = \pm q_e \tag{A8b}$$

Third, the barrier height $V^{\ddagger}$ is fixed at $q = 0$; thus

$$V_0 = V^{\ddagger} \tag{A8c}$$

Fourth, the resulting energy gap $E_2 - E_0$ of vibrational states $|2\rangle$ and $|0\rangle$ is set to the photon energy of the fundamental transition

$$E_2 - E_0 = \hbar\omega \tag{A8d}$$

(For the choice of levels $|2\rangle$, $|0\rangle$, not $|1\rangle$, $|0\rangle$, see section 2.)

Fifth, we specify the widths of the double-well potential by choosing the appropriate force constant k at the bottoms of the potential wells

$$\partial^2 V/\partial q^2 = k \text{ at } q = \pm q_e \tag{A8e}$$

For the application of the present model, we adopt typical values q_e, $V^{\ddagger}$, and $\hbar\omega$ from experimental results for the normal isotopomers of semibullvalenes where C = ^{12}C and H = ^{1}H. Specifically, we use $q_e/a_0 = 0.62$,[21] $V^{\ddagger}$/kJ mol^{-1} = 25,[22] and $\hbar\omega$/cm^{-1} = 900.[23] For the last parameter, k in eq A8e, there is no direct experimental reference. Therefore, we consider two rather arbitrary yet characteristic cases yielding narrow (n) or broad (b) potential wells. The corresponding five parameters satisfying five conditions (see eqs A8a–e) are listed in Table I for V_b and V_n. The resulting potentials $V(q) = V_b(q)$ or $= V_n(q)$ are shown in Figures 1 and 2, respectively, together with the vibrational energies E_v and wave functions $\Psi_v(q)$. Note that, indeed, both potentials $V_b(q)$ and $V_n(q)$ yield identical minima (see eq A8a,b), barrier heights (see eq A8c), and fundamental frequencies (see eq A8d),

---

(21) The value of q_e should be slightly larger than the difference of the equilibrium bond lengths (C3 – C4) – (C1 – C2) (Scheme II), depending on the centers of masses of the bonds (C_i – H_i); see eq A2. The explicit evaluation of this dependence would even enhance the inverse isotope effect; see section 3. Nevertheless, for the sake of simplicity, we employ a fixed value, q_e = 33 pm, in the range of typical experimental values, e.g., (226.1–160.0) pm for the parent semibullvalene, as determined by electron diffraction analysis; see: Wang, Y. C.; Bauer, S. H. *J. Am. Chem. Soc.* **1972**, *94*, 5651–5657, or for substituted semibullvalenes as determined by X-ray diffraction; see: Quast, H.; Carlsen, J.; Janiak, R.; Peters, E.-M.; Peters, K.; von Schnering, H. G. *Chem. Ber.* **1992**, *125*, 955–968.

(22) Arrhenius activation energies of 21.3 ± 0.8[4a] and 23.2 ± 0.4 kJ mol^{-1}[4b] for the degenerate Cope rearrangement of the parent semibullvalene have been determined by nuclear magnetic resonance spectroscopy.

(23) The temperature dependence of the UV spectrum of 2,6-dicyano-1,5-dimethylsemibullvalene is indicative of an equilibrium between the vibrational ground state and another species, higher in energy by 10.7 kJ mol^{-1} $\simeq$ 894 cm^{-1}, which may be regarded as a vibrationally excited state: Quast, H.; Christ, J. *Angew. Chem., Int. Ed. Engl.* **1984**, *23*, 631–632. Quast, H.; Geissler, E.; Mayer, A.; Jackman, L. M.; Colson, K. L. *Tetrahedron* **1986**, *42*, 1805–1813.

J. Am. Chem. Soc. 1993, 115, 1495-1500

but different widths or force constants (see eq A8e).

We like to add that we have also tried less flexible potential functions, e.g., fourth- or sixth-order polynomials $V(q) = V_0 + V_2q^2 + V_4q^4$ $(+V_6q^6)$, but these cannot account for the "experimental" conditions (see eqs A8a–d), irrespective of the value of k in eq A8e. However, other functions with less parameters would also satisfy conditions (see eqs A8a–d), e.g., a double Morse potential

$$V = D\{\exp[-(-q + q_e)\beta] - 1\}^2 + D\{\exp[-(q + q_e)\beta] - 1\}^2 - D \quad \text{(A9)}$$

with parameters $D = 0.0098E_h$, $q_e = 0.62a_0$, $\beta = 8.4a_0^{-1}$, yielding $V^* = 25$ kJ mol^{-1} and $\hbar\omega = 900$ cm^{-1} and $V(q_e) = V(-q_e) \cong 0$. This double Morse potential would also account for the inverse isotope effect; i.e., $\hbar\omega$ would increase from 900.0 cm^{-1} to 920.4 cm^{-1} when $^{12}C^1H$ is replaced by $^{13}C^2H$.

Finally, let us consider the symmetry selection rules for the fundamental transition $|0\rangle \rightarrow |2\rangle$ depending on the dipole functions $\mu_i(q)$, $i = x, y, z$ and matrix elements $\langle 2|\mu_i|0\rangle$.

The C_s symmetry of semibullvalene along the reaction path q implies the following symmetries of the μ_i's (see Scheme I):

$$\mu_x(q) = -\mu_x(-q) \quad \text{(A10a)}$$

$$\mu_y(q) = 0 \quad \text{(A10b)}$$

$$\mu_z(q) = +\mu_z(-q) \quad \text{(A10c)}$$

For the resulting matrix elements of levels $|0\rangle$, $|2\rangle$ with gerade symmetry, we obtain

$$\langle 2|\mu_x|0\rangle = 0 \quad \text{(A11a)}$$

$$\langle 2|\mu_y|0\rangle = 0 \quad \text{(A11b)}$$

$$\langle 2|\mu_z|0\rangle \neq 0 \quad \text{(A11c)}$$

As a consequence, we have

$$\langle 2|-\mu E|0\rangle = -\langle 2|\mu_z|0\rangle E_z \quad \text{(A11d)}$$

for the dipole transition matrix element, and the golden rule for the rate of absorption

$$k(2 \leftarrow 0) = (2\pi/\hbar)\langle 2| - 0.5\mu \times E|0\rangle^2\delta(E_2 - E_0 - \hbar\omega) \quad \text{(A12)}$$

calls for z-polarized light

$$E_z = E\exp[i(k_zz - \omega t)] \quad \text{(A13)}$$

otherwise, the fundamental transition $|0\rangle \rightarrow |2\rangle$ is dipole-forbidden.

Neural Network Classification of Inductive and Resonance Effects of Substituents

Vladimír Kvasnička,* Štěpán Sklenák, and Jiří Pospíchal

Contribution from the Department of Mathematics, Faculty of Chemical Technology, Slovak Technical University, 81237 Bratislava, Czechoslovakia. *Received June 10, 1992*

Abstract: An application of feed-forward neural networks adapted by back-propagation strategy to classification of inductive and resonance effects of functional groups is described. The descriptors of functional groups, forming the input information to the neural network, are determined as numbers of times certain subgraphs (with evaluated vertices and edges) appear in the functional group under study. The hidden activities are used for cluster analysis of functional groups.

Introduction

Neural networks[1,2] are equipped by learning features that allow computers to be trained to recognize patterns in data of high dimensionality. Such patterns are manifested by effective correlations between molecular structure and property.[3-5] The neural networks do not require any formulation of rules about reactivity to make decisions. They form an internal model by extracting information directly from the properly selected examples belonging to the so-called training set. The expert systems based on neural networks can be used to roughly estimate the yields of reactions and to classify the reaction products (e.g., regioselectivity). Such an expert system is vital in any computer system for organic synthesis design.

The purpose of the present communication is to demonstrate an application of neural networks for classification and prediction of inductive and resonance effects (represented by σ constants) of functional groups. These parameters, initially introduced in physical organic chemistry,[6] describe the influence of functional groups on the reactivity of synthons[7,8] (reaction cores). Input information to the neural network, which properly represents the topology and basic physical parameters of functional groups, was chosen to consist of simple descriptors[5,9] assigned to numbers of appearance of specially labeled rooted subgraphs in the functional group. This means that the functional groups are described by graph-theoretical parameters without the necessity to calculate any additional physical or physico-chemical parameters of functional groups. The results obtained are very encouraging and

---

(1) (a) Simpson, P. K. *Artificial Neural Systems*; Pergamon Press: New York, 1990. (b) Wasserman, P. *Neural Computing: Theory and Practice*; Van Nostrand Reinhold: Princeton, NJ, 1989.

(2) Rumelhart, D. E.; McClelland, J. L. (and the PDP Research Group) *Parallel Distributed Processing*; MIT Press: Cambridge, MA, 1986; Vols. I and II.

(3) (a) Župan, J.; Gasteiger, J. *Anal. Chim. Acta* **1991**, *248*, 1. (b) *Tetrahedron Comput. Methodol.* **1990**, *3*, no. 1.

(4) (a) Elrod, D. W.; Maggiora, G. M.; Trenary, R. G. *J. Chem. Inf. Comput. Sci.* **1990**, *30*, 477. (b) Elrod, D. W.; Maggiora, G. M.; Trenary, R. G. *Tetrahedron Comput. Methodol.* **1990**, *3*, 163. (c) Luce, H. H.; Govind, R. *Tetrahedron Comput. Methodol.* **1990**, *3*, 143.

(5) Kvasnička, V.; Pospíchal, J. *J. Mol. Struct.* (*THEOCHEM*) **1991**, *235*, 227.

(6) Hammett, L. P. *Physical Organic Chemistry*; McGraw-Hill: New York, 1970.

(7) Corey, E. J. *Pure Appl. Chem.* **1967**, *14*, 19.

(8) (a) Kvasnička, V.; Pospíchal, J. *Int. J. Quant. Chem.* **1990**, *28*, 253. (b) Koča, J.; Kratochvíl, M.; Kvasnička, V.; Matyska, L.; Pospíchal, J. *Synthon Model of Organic Chemistry and Synthesis Design*. Springer Verlag: Berlin, 1989.

(9) Zou, Y.; Johnson, M.; Tsai, C.-C. *J. Chem. Inf. Comput. Sci.* **1990**, *30*, 442.

0002-7863/93/1515-1495$04.00/0